

# Thermophysical Comparison of Five Commercial Paraffin Waxes as Latent Heat Storage Materials

N. Ukrainczyk,\* S. Kurajica, and J. Šipušić

University of Zagreb, Faculty of Chemical Engineering and Technology,  
Marulićev trg 19, HR-10000 Zagreb, Croatia

Original scientific paper

Received: April 15, 2009

Accepted: December 28, 2009

Thermophysical properties of phase change materials (PCM) are of utmost importance in latent heat thermal energy storage (LHTES) applications. Therefore, an experimental study is conducted in order to determine thermophysical properties of five technical grade paraffin waxes produced by major Croatian oil company, INA d.d. Rijeka. The temperatures and enthalpies of melting and solidification (latent heat capacity) and specific heat capacities of solid and liquid paraffin waxes were measured by differential scanning calorimetry (DSC). The thermal diffusivity of paraffin waxes was determined utilizing transient method. The importance of eliminating phase transformation interferences to thermophysical properties determination is addressed. The densities and the coefficient of thermal expansion were measured using Archimedes methods. A self-adopted simple and inexpensive laboratory procedure for the determination of liquid density as a temperature function is presented. Finally, the thermal conductivities have been calculated from measured densities, heat capacities and diffusivities. Based on results obtained, the investigated paraffin waxes were evaluated in regard to their applicability as PCM for LHTES.

*Key words:*

Paraffin wax, phase change material, latent heat thermal energy storage, thermophysical properties

## Introduction

The basic problem in utilization of thermal systems is the discrepancy between energy availability and its demand. For example, because of the periodic nature of solar radiation as well as ambient temperature, natural heating is more effective if daily excessive heat is stored into the suitable accumulation system for latter use. In order to enhance the applicability, performance, and reliability of thermal systems, latent heat thermal energy storage (LHTES) methods<sup>1</sup> are used. In a LHTES, energy is stored during melting and recovered during solidification of the phase change material (PCM), mostly by means of latent heat of phase change of the medium. PCM should have high storage density, i.e. high latent heat of phase transition and high density to provide a higher thermal storage per unit mass, high specific heat capacity to provide sensible heat storage and small temperature variation from storage to retrieval.<sup>1</sup> A large number of materials, inorganic and organic and their mixtures have been investigated as LHTES materials.<sup>2</sup> Recently, Kurajica<sup>3</sup> presented a short review on phase change (latent heat storage) materials and systems. Numerous applications of PCMs, e.g. in building, air and water conditioning, heat sinks etc. had been reviewed by Zalba.<sup>4</sup>

Paraffin waxes are the most commonly used commercial organic heat storage PCM<sup>5</sup> used for LHTES applications due to their large latent heat, moderate thermal energy storage density, little or no undercooling, low vapor pressure, good thermal and chemical stability, lack of phase separation, self-nucleating behavior, varied phase change temperatures (i.e. they can meet the requirements of a desired LHTES application), environmental harmlessness, having no unpleasant odor, non-toxicity and low price.<sup>5</sup> Several investigations of thermal characteristics of pure paraffins and paraffin waxes during solidification and melting processes have been performed, showing that no thermal properties degradation occurred after numerous melting/freezing cycles.<sup>6–8</sup> Their major drawback is low thermal conductivity ( $\lambda \sim 0.2 \text{ W m}^{-1} \text{ K}^{-1}$ ), decreasing the rates of heat storage and release during melting and crystallization operations (requiring large surface area), flammability and density changes.<sup>9</sup> The changes in density in the course of heating/cooling to a melting/solidification temperature, as well as the solid/liquid phase transformation inflict great volume change.

Paraffins are a family of saturated hydrocarbons with general formula  $C_nH_{2n+2}$ . Paraffins having between 5 and 15 carbon atoms are liquids at room temperature, and those with more carbon at-

\*Corresponding author: N. Ukrainczyk, nukrainc@fkit.hr

oms are waxy solids (e.g. well-known paraffin octadecane,  $C_{18}H_{38}$ ).<sup>10</sup> Paraffin can be classified according to purity, i.e. refinement, melting point, etc. Considering the cost, however, only technical grade paraffin wax, a by-product of oil refining, may be used as PCM in latent heat storage. Commercial grade paraffin waxes are combination of different, mainly straight chain, hydrocarbons with more than 15 carbon atoms having melting temperatures<sup>11</sup> ranging from 23 to 67 °C. The various paraffin waxes, byproducts of oil refining, therefore easily available and cheap, are obtainable in a selection of melting point ranges, so that a good match can be made between melting range and system operating temperature.

Generally, the longer the length of the pure hydrocarbon chain is, the greater are the melting temperatures and specific heat of fusion, densities and molar specific heat capacities (of liquid and solid).<sup>5</sup> An overview of various properties of interest for utilization of paraffin waxes as LHTES materials is given in Table 1.

The thermophysical properties presented in Table 1<sup>11–21</sup> represent ranges of values due to the incomplete data and scarce studies relating interdependence of thermophysical properties.<sup>22</sup> Furthermore, large differences exist between values reported in different studies, e.g.<sup>11–13</sup> for solid thermal conductivities of even above 100 %. Some authors<sup>23</sup> reported that the thermal conductivity of

paraffin wax, in solid phase, was not a monotonic function of temperature. The variations in conductivity, density and enthalpy against temperature for some paraffins are documented by Manoo and Hensel.<sup>24</sup> Reported non-monotonic temperature functions of these properties are probably due to the phase change transitions, especially the solid-solid transitions.

Moreover, the data on liquid paraffin waxes thermal properties and especially their dependence on temperature are particularly scarce in available literature.

Therefore, in order to acquire data necessary for further investigations of the employment of paraffin waxes as PCM for LHTES medium, as well as for the dimensioning of LHTES equipment, thermal and thermal performance related properties of five paraffin waxes produced by INA d.d., Croatia have been studied. The melting/solidification temperatures, enthalpies of melting and solidifying of paraffin waxes, specific heat capacity, thermal diffusivity and the density in solid and liquid state were measured. Based on data obtained, the thermal conductivity was calculated and the investigated paraffin waxes were evaluated in regard to their applicability as PCM for LHTES.

The described transient method is, to the best of our knowledge, applied for the first time for determination of thermal diffusivity of paraffin waxes. As the solid/liquid phase transformation inflicts

Table 1 – Thermophysical properties of paraffin wax

Paraffin type	Melting/°C	Heat of fusion/J g <sup>-1</sup>	$\lambda/W\ m^{-1}\ K^{-1}$	$\rho/g\ cm^{-3}$	$c_p/J\ g^{-1}\ K^{-1}$	$a/10^{-7}\ m^2\ s^{-1}$
C18	28 <sup>11</sup>	244 <sup>11</sup>	0.148 (l, 40 °C) <sup>12</sup>	0.774 (l, 70 °C) <sup>11</sup>	n.a.	n.a.
	27.5 <sup>12</sup>	243.5 <sup>12</sup>	0.15 (s) <sup>11</sup>	0.814 (s, 20 °C) <sup>11</sup>		
			0.358 (s, 25 °C) <sup>12</sup>			
C20–C33	48–50 <sup>11</sup>	189 <sup>11</sup>	0.21 (s) <sup>11</sup>	0.769 (l, 70°C) <sup>11</sup>	n.a.	n.a.
				0.912 (s, 20 °C) <sup>11</sup>		
C22–C45	58–60 <sup>11</sup>	189 <sup>11</sup>	0.21 (s) <sup>11</sup>	0.795 (l, 70 °C) <sup>11</sup>	n.a.	n.a.
				0.920 (s, 20 °C) <sup>11</sup>		
Paraffin wax	64 <sup>13,14</sup>	173.6 <sup>13,14</sup>	0.167 (l, 63.5 °C) <sup>13,14</sup>	0.790 (l, 65 °C) <sup>13,14</sup>	n.a.	n.a.
		266 <sup>15</sup>	0.346 (s, 33.6 °C) <sup>13,14</sup>	0.916 (s, 24 °C) <sup>13,14</sup>		
			0.339 (s, 45.7 °C) <sup>14</sup>			
C21–C50	66–68 <sup>11</sup>	189 <sup>11</sup>	0.21 (s) <sup>11</sup>	0.830 (l, 70 °C) <sup>11</sup>	n.a.	n.a.
				0.930 (s, 20 °C) <sup>11</sup>		
C19–C36	48–68 <sup>16,17</sup>	147–163 <sup>18</sup>	0.23 (s, 25 °C) <sup>19</sup>	0.766–0.770 (l, 82 °C) <sup>20</sup>	2.981 (l, 60–63 °C) <sup>18</sup>	0.97–1.02*
				0.865–0.913 (s, 25 °C) <sup>18,19</sup>	2.604 (s, 35–40 °C) <sup>18</sup>	
Paraffin wax <sup>21</sup>	53	184.48	0.15 (s)	0.775 (l)	2.384 (s)	n.a.

\*Calculated range based on the literature data.

(s) – solid, (l) – liquid

n.a. – not available

great volume change, a special pretreatment was applied to the transient method to obtain a homogeneous sample. Furthermore, a methodology was developed to eliminate errors of thermal diffusivity and heat capacity measurements due to phase change transitions, previously inadequately addressed in literature. Temperature dependence of liquid densities of the investigated paraffin waxes is measured by a self-adopted simple laboratory procedure.

## Experimental

### Materials

Commercial paraffin waxes, denoted by the manufacturer as 46–50, 52–54, 58–62, 62–70 and 70–75, were obtained from INA, Rijeka, Croatia. The samples were used as received.

### DSC analysis

Thermal properties of paraffin waxes such as melting and solidification temperatures, latent heats of melting and solidification and heat capacities were measured by differential scanning calorimetry (DSC) technique. DSC was performed on a Thermal Analyzer DSC 2910, TA Instruments in heating and cooling cycle. Samples with a mass of ~5 mg were sealed in an aluminum pan; an empty pan was used as reference. The analyses were performed in the temperature range of –20–90 °C with a heating rate of 5 °C min<sup>-1</sup> and under a constant stream of nitrogen at a volume flow rate of  $Q = 100 \text{ mL min}^{-1}$ . Before the DSC runs, the samples were heated to 90 °C for 30 min in order to eliminate the thermal memory effect. Indium was used for temperature ( $T_f = 429.75 \text{ K}$ ) and specific enthalpy ( $\Delta h_f = 28.62 \text{ J g}^{-1}$ ) calibration, while  $\alpha\text{-Al}_2\text{O}_3$  was used as a reference for heat capacity determination. The specific heat capacity was obtained from three DSC measurements: a sample, a baseline, and a reference. The baseline data is used for baseline subtraction from the reference and sample data. The reference data provided a temperature dependent calibration constant. Cooling was accomplished with a liquid-nitrogen cooling accessory. The solid-solid transition, melting and solidification temperatures were obtained by drawing a line at the point of maximum slope of the leading edge of the DSC peak and extrapolating a base line on the same side as the leading edge of the peak. The heats of fusion of investigated materials were determined by numerical integration of the peak area of the peak of thermal transition.

### Thermal diffusivity measurement setup

Thermal diffusivity ( $a/\text{m}^2 \text{ s}^{-1}$ ) is an important property of material in all problems involving transient heat conduction. It is a measure of rapidity of the heat propagation through a material and combines thermal conductivity ( $\lambda$ ), specific heat capacity ( $c_p$ ) and density ( $\rho$ ) according to:

$$a = \frac{\lambda}{\rho c_p} \quad (1)$$

Transient heat conduction in the radial direction in an infinite cylinder can be expressed as:<sup>25</sup>

$$\frac{1}{a} \frac{\partial T}{\partial t} = \frac{\partial^2 T}{\partial r^2} + \frac{1}{r} \frac{\partial T}{\partial r} + \frac{\varphi}{\lambda} \quad (2)$$

where  $\varphi$  is a volumetric heat generation or sink term ( $\text{W m}^{-3}$ ). For the case of investigated material this term is associated with phase transformations. In order to obtain accurate measurements of thermal diffusivity, a methodology assuring the elimination of errors due to simultaneous phase change transitions was applied.

For thermal diffusivity measurements, an experimental transient method was used.<sup>26–28</sup> An experimental setup consisted of a two constant-temperature water baths ( $\vartheta \pm 0.03 \text{ }^\circ\text{C}$ ), the PCM storage copper cylinder container, K-type thermocouples wiring, data acquisition unit and a PC, Fig. 1. The copper tube with 26 mm diameter, 170 mm length and 0.7 mm thickness was filled with liquid paraffin wax and the thermocouple was placed in the

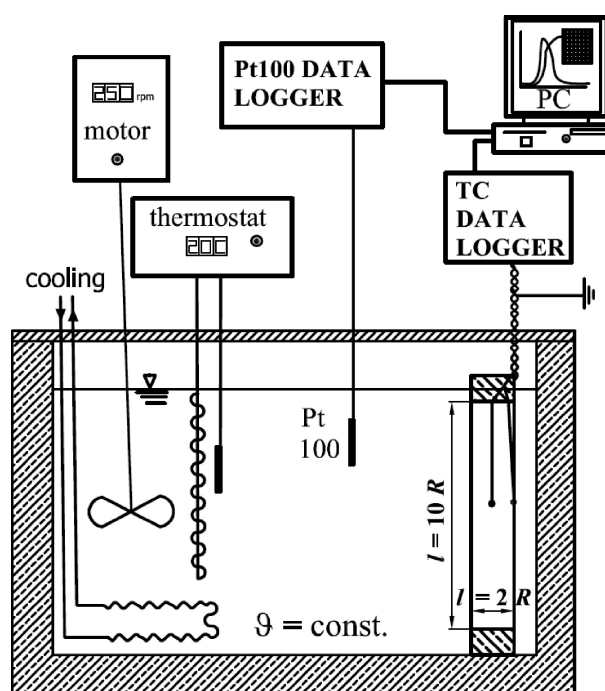


Fig. 1 – Thermal diffusivity measuring set-up

center of the cylinder at half-length. The specimen geometry assured one-dimensional heat transfer. Copper tube was sealed with rubber stoppers. Phase change from liquid to solid resulted in considerable volume contraction. Therefore, in order to avoid the creation of air gaps and assure sample homogeneity, rubber stoppers were continuously pressed during paraffin wax solidification upon cooling. The cylinder was placed vertically in the bath cooled to a temperature  $\vartheta = 5\text{ }^{\circ}\text{C}$  and held there until temperature equilibration. Then the cylinder was suddenly immersed in the bath at temperature  $\vartheta = 10\text{ }^{\circ}\text{C}$  and held until temperature equilibration. The temperature of the paraffin wax at a cylinder axis was measured as a function of time. The sudden immersion provided an approximate step-like temperature inducement at the copper cylinder container  $\vartheta(r = R, t)$ . Boundary temperature increase was measured at the inside surface of the copper tube wall. The transient temperature response was measured at the center of the paraffin wax cylinder  $\vartheta(r \sim 0, t)$ . At the end of the series of experiments, the paraffin wax sample was pushed out from the tube after short warming in a hot bath. Then the accurate radial position of the thermocouple measuring end was obtained and the sample was checked for the homogeneity.

K-type thermocouples, 0.2 mm thick, with grounded twisted-shielded wiring were used to obtain accuracy and eliminate noise. Cable shielding and twisted wire pairs were used to minimize or eliminate capacitive coupled interference and to aid in lowering electromagnetically induced errors. The thermocouples were calibrated before use (using Pt 100 with an overall measuring accuracy of  $\vartheta \pm 0.03\text{ }^{\circ}\text{C}$ ), and they were observed to have an accuracy of  $\vartheta \pm 0.1\text{ }^{\circ}\text{C}$  in a temperature range  $\vartheta = 0\text{--}90\text{ }^{\circ}\text{C}$ . An 8-channel data logger (TC-08 pico technology) was used for temperature measurements. The 20-bit resolution ensured detection of minute changes in temperature. It was capable of storing the entire set of temperatures once every 100 ms. The experimental data were simultaneously transferred to a PC. Cold junction temperature held at room temperature was sensed by a precision thermistor in good thermal contact with the input connectors (on thermal block) of the measuring instrument. In order to have an accurate cold junction compensation, its temperature change was kept as low as possible.

Based on the described experimental transient method the thermal diffusivity can be estimated by fitting the experimental results to a theoretical expression based on a Bessel function<sup>29</sup> or its linear (first term) approximation.<sup>26</sup> However, in this work a numerical approach for parameter estimation was adopted for better accuracy. Instead of assuming an ideal step temperature inducement, a real measured

temperature was employed for the boundary condition. Fourier's one dimensional radial heat eq. (2) was solved using Matlab's built-in solver "pdepe".<sup>30,31</sup> The heat generation term was neglected (please, see further discussion on this issue below). The Levenberg-Marquardt method for optimization was used for the solution of the inverse problem of the parameter estimation.<sup>27</sup> The inverse problem was solved and optimized by using a sub-program that was written for the setting of Matlab 6.5 (The MathWorks, Inc., Natick, MA); (.m) script files are freely available upon request to a corresponding author. Inputs for this numerical model were temperature-time vectors, i.e.  $\vartheta(r = R, t)$  and  $\vartheta(r \sim 0, t)$ , and the initial condition  $\vartheta(r, t = 0)$ . In order to speed up the iterative computing, the temperature-time input was reduced as follows. First, the accurate onset of inducement was determined from raw temperature data (collected each 100 ms). Then, the temperature records were reduced to about 1000 time points for each measurement position.

The results of the method evaluation on reference materials indicated an accuracy of 1 % and a precision of 0.7 % (for 95 % confidence).<sup>27</sup> The reference materials used to evaluate the method and the apparatus were gelatinous water (Agar gel 0.7 %), glycerol (p.a. redistilled) and Ottawa (quartz) sand.

### Density measurements

The densities of solid samples were determined by applying classical Archimedes method. The densities of liquid samples were measured by the self-adopted simple laboratory procedure utilizing Archimedes law in the following experimental setup shown in Fig. 2. A preheated laboratory glass with liquid paraffin wax was placed in a preheated Dewar vessel, sealed with a thermal insulating stopper. A thermocouple was introduced in Dewar vessel through a small hole in a stopper. When a pre-

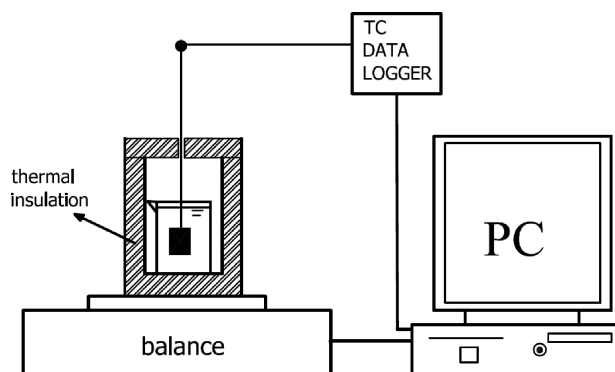


Fig. 2 – Self-adopted simple and inexpensive laboratory procedure for the determination of liquid density as a function of temperature

heated sinker (59.534 cm<sup>3</sup>), tied up by a thin wire was immersed in a liquid paraffin wax, the mass was recorded. During slow cooling, for about 24 h, mass and temperature were simultaneously measured using balance data output and the temperature sensor connected to a computer. That way, the density of liquid paraffin wax as a function of temperature was determined.

## Results and discussion

### DSC measurements, transition temperatures and cumulative heat of phase transformations

The DSC curves of investigated samples are shown in Fig. 3. In DSC thermograms, the main (sharp) peaks represent solid–liquid (melting) or liquid–solid (solidification) phase change and the minor peak (or peaks) to the left of the main peak correspond to solid–solid phase transitions.<sup>32</sup> According to the literature,<sup>33</sup> on heating, prior to isotropization to the melt, some paraffin waxes display transitions due to a disordering of the monoclinic crystal to a pseudohexagonal crystal. The increase in melting and freezing points among the investigated samples is a consequence of change in composition of paraffin waxes since the melting point of the paraffins increases with the increased number of carbon atoms in paraffin chain.<sup>10</sup> However, it has to be pointed out that the phase changes take place over a temperature range. From Fig. 3 it can be seen that the sample undercooling is small, even at employed heating/cooling rate 5 K min<sup>-1</sup> the difference between melting/solidification curves is less than 6 K.

For the mathematical modeling of the LHTES material thermal response, the enthalpy of phase transformation term in eq. (2) is commonly introduced by an apparent heat capacity methodology.<sup>34</sup> This takes into account the temperature range over

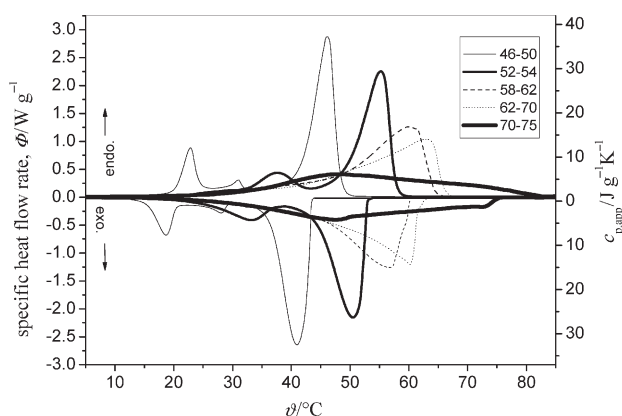


Fig. 3 – The DSC thermograms and apparent specific heat capacities of paraffin waxes 46–50, 52–54, 58–62, 62–70 and 70–75 obtained with the heating and cooling rate of 5 K min<sup>-1</sup>

which the phase transition occurs. A characteristic of fully miscible mixtures is that the phase change occurs in a temperature range instead at a fixed temperature, as it does for pure substances. An assumption that the melting or solidification occurs at constant temperature leads to a greater discrepancy between experimental and numerical results.<sup>34</sup> The shape of the effective heat capacity function depends significantly on the heating and cooling rates used in the measurements and sample size. Frequently, the enthalpy function or the effective heat capacity of the PCM is determined on the basis of DSC measurements. From the measured heat flow,  $\Phi(T)$ , and specific heat capacity of solid or liquid PCM,  $c_p$ , the apparent heat capacity is calculated.

$$c_{p,app}(T) = \frac{\Phi(T)}{m\dot{T}} + c_p \quad (3)$$

where  $m$  is the mass of PCM used in DSC experiment,  $\dot{T}$  is heating or cooling rate of the DSC measurement and  $\Phi(T)$  is heat flow rate. Apparent heat capacities of the samples 46–50, 52–54, 58–62, 62–70 and 70–75 are presented in Fig. 3 on the right axis. According to Fig. 3 it is obvious that for the investigated samples no simple function for the description of apparent heat capacity over the whole temperature range exist.

In Fig. 4 the cumulative heats of solid–solid and solid–liquid transformations are presented. Samples 46–50 and 52–54 show solid–solid transition(s) which increase their total enthalpy change. Closer inspection of the low temperature side of DSC peaks of samples 58–62 and 62–70 also reveals the presence of additional transition. The increase in heat of fusion is expected because of the presence of longer-chain paraffines.<sup>5</sup> The comparison is not straightforward, since the heats of solid–solid transformations and fusion could not be

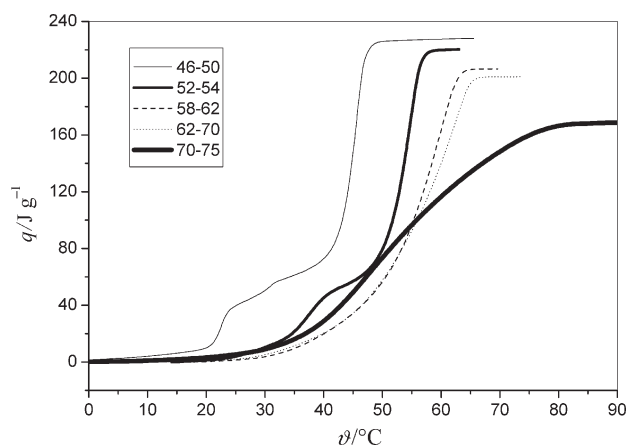


Fig. 4 – Cumulative heats (sensible heat plus latent heat of phase transformations) of paraffin waxes 46–50, 52–54, 58–62, 62–70 and 70–75, determined by numerical integration of the melting DSC peak areas

separated. It seems that the heats of fusion are approximately the same for samples 46–50 and 52–54, the same is valid for samples 58–60 and 62–70 which show some increase compared to the first two samples. The lowest heat of fusion is exhibit by sample 70–75. Such behavior is probably due to an increasing complexity of the paraffin mixture, enabling only partial crystallization to occur. From the heat flow signal, three characteristic temperatures for each transition can be determined: the transition temperature,  $\vartheta_t$  (temperature corresponding to separation of the DSC heat flow curve from the base in the course of heating), melting temperature,  $\vartheta_m$  (temperature corresponding to onset of the DSC melting peak) and the solidification temperature,  $\vartheta_s$  (temperature corresponding to separation of the DSC heat flow rate curve from the base line in the course of cooling). Table 2 shows the characteristic transition, melting and solidification temperatures, and total enthalpy change of the investigated samples.

Table 2 – Transition temperature ( $\vartheta_t$ ), melting temperature ( $\vartheta_m$ ), solidification temperature ( $\vartheta_s$ ) and cumulative heat (sensible heat plus latent heat of phase transformations), ( $q$ ) of investigated paraffin waxes

Sample	46–50	52–54	58–62	62–70	70–75
$\vartheta_t/^\circ\text{C}$	20, 28	20, 32	27	25	–
$\vartheta_m/^\circ\text{C}$	41	49	46	37	30
$\vartheta_s/^\circ\text{C}$	43	53	60	62	75
$q/\text{J g}^{-1}$	228	220	206	201	169

### Heat capacities

Heat capacities of the solid and liquid samples 46–50, 52–54, 58–62, 62–70 and 70–75 at  $\vartheta = 7.5$  and  $80^\circ\text{C}$  are presented in Fig. 5 and Table 3. Specific heat capacities of solid and liquid are extracted from Fig. 3, within a temperature range chosen in a manner to minimize influence of phase transitions. The values at  $\vartheta = 7.5^\circ\text{C}$  and  $80^\circ\text{C}$  are given in Table 3. Heat capacities of liquid paraffin waxes show higher values than the corresponding solids, which is in good agreement with literature.<sup>5,18</sup> The higher heat capacity of liquids than solids can be attributed to a higher degree of freedom for vibrations of hydrocarbon chains and to the energy used for overcoming of the van der Waals attractive forces. The magnitude of obtained values are somewhat higher but in reasonable agreement with data for C18–C50 *n*-alkanes,<sup>5</sup> which range from 1.7 to  $2.0 \text{ J g}^{-1} \text{ K}^{-1}$  for solids and 2.3 to  $2.4 \text{ J g}^{-1} \text{ K}^{-1}$  for liquids. Higher values of heat capacities of mixtures

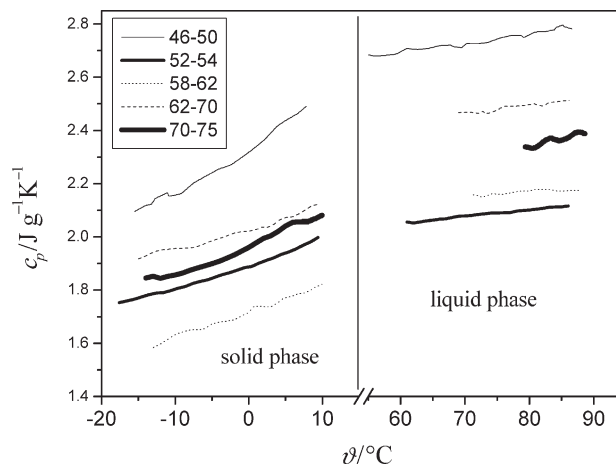


Fig. 5 – Specific heat capacity of solid and liquid paraffins obtained by DSC (an extraction of Fig. 3)

Table 3 – Results on investigated paraffin wax samples: specific heat capacity of solid and liquid, thermal diffusivity, the densities of paraffin wax samples at  $\vartheta = 7.5^\circ\text{C}$  and  $\vartheta = 80^\circ\text{C}$ , corresponding specific volumes and relative volume change in selected temperature interval, and thermal conductivity calculated using eq. (1)

Sample	46–50	52–54	58–62	62–70	70–75
$c_p(s, 7.5^\circ\text{C})/\text{J g}^{-1} \text{ K}^{-1}$	2.48	1.97	2.10	1.82	2.06
$c_p(l, 80^\circ\text{C})/\text{J g}^{-1} \text{ K}^{-1}$	2.76	2.10	2.49	2.17	2.34
$a(5\text{--}10^\circ\text{C})/10^{-7} \text{ m}^2 \text{ s}^{-1}$	1.03	1.08	1.11	1.12	1.13
$\rho(s, 7.5^\circ\text{C})/\text{g cm}^{-3}$	0.829	0.866	0.893	0.911	0.917
$\rho(l, 80^\circ\text{C})/\text{g cm}^{-3}$	0.765	0.774	0.782	0.799	0.822
$v_{7.5}/\text{cm}^3 \text{ g}^{-1}$	1.206	1.155	1.120	1.098	1.091
$v_{80}/\text{cm}^3 \text{ g}^{-1}$	1.307	1.292	1.279	1.252	1.217
$\Delta v/\%$	7.7	10.6	12.4	12.3	14.8
$\lambda(s, 7.5^\circ\text{C})/\text{W m}^{-1} \text{ K}^{-1}$	0.21	0.19	0.21	0.19	0.21

in comparison to pure *n*-alkanes were also documented by literature,<sup>18</sup> Table 1, row 6. Contrary to the molar heat capacities of liquids and solids, the mass specific heat capacities have no monotonic correlation with the length of the hydrocarbon chain.<sup>5</sup>

The increase of heat capacity with temperature is more pronounced for the solids than the liquids, Fig. 5. This can be attributed to the gradual onset of molecular rotational freedom (rotation of the whole molecules about their long axis)<sup>35</sup> and to heterophase premelting.

Finke *et al.*<sup>35</sup> also observed an abnormal increase in heat capacities below the melting temperatures on pure *n*-alkanes (C8–C16).

### Thermal diffusivity

Measurements of thermal diffusivity are conducted within a temperature range chosen in a manner to minimize interferences of phase transformations. These temperatures were selected by referring to DSC results, Fig. 3. In that way, enthalpy of phase transformation term in eq. (2) is eliminated, enabling reasonably accurate estimation of investigated properties.

An example of thermal diffusivity estimation, based on the measured temperature response (specimen 46–50) and the radial heat conduction model in eq. (2), is given in Fig. 6. A good fit with a standard deviation  $\sigma \sim 1.7 \cdot 10^{-2} \text{ }^\circ\text{C}$  indicates no significant heat of fusion interference to measurement.

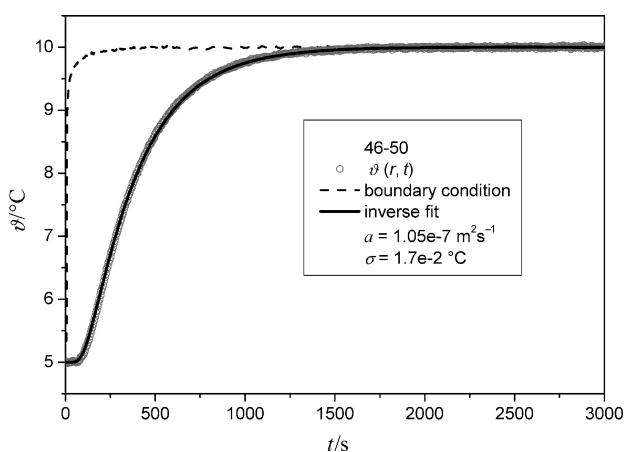


Fig. 6 – An example of the estimation of thermal diffusivity based on the measured temperature response (specimen 46–50) and the radial heat conduction model in eq. (2)

Results on thermal diffusivities are given in Table 3, and represent an average value of five measurements with a measurement uncertainty of 1.5 % (for 95 % confidence level). Since measured data on thermal diffusivity of paraffin waxes is scarce, the obtained values were compared with calculated values (Table 1, row 6) and a reasonable agreement has been obtained. An increase of thermal diffusivities with melting temperatures of investigated paraffin waxes is observed.

### Density measurements

It is known from the literature<sup>36</sup> that paraffins show great volume changes on heating, solid-solid transformations and solid-liquid phase change. The volume changes have significant effects on the application technology. Therefore, in order to provide data on volume changes, as well as to provide data on densities necessary for the thermal conductivity calculation, the investigation of wax density in solid and liquid state has been conducted. Com-

puter-control measurement setup enabled very accurate measurements. The densities of solid and liquid samples at selected temperatures are presented in Table 3. The changes in density of liquid paraffin wax samples with the temperature are presented in Fig. 7. All melted samples exhibited a constant decrease of density, i.e. constant rise in volume with temperature. It is interesting to note that the slope obtained by linear regression is decreasing with the increasing melting temperatures of investigated paraffin waxes. The results obtained for liquids and solids in this work follow the correlation reported on pure hydrocarbons, i.e. the longer the average length of the hydrocarbon chain is, the greater are the densities of liquids and solids.<sup>5</sup> Obtained values for liquid and solid paraffin waxes are in reasonable agreement with data in Table 1.

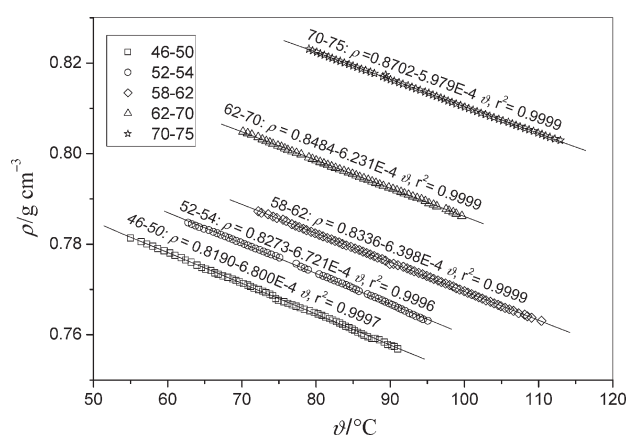


Fig. 7 – Densities of liquid paraffin wax samples as a function of temperature ( $\bar{\vartheta}$  in  $^\circ\text{C}$ )

Using density data, the volume changes has been calculated in the temperature interval of interest and are presented in Table 3. The wax specific volumes at 7.5  $^\circ\text{C}$  and 80  $^\circ\text{C}$  have been taken as reciprocal density. The volume change during the phase change process has been calculated using equation:

$$\Delta\nu = \frac{\nu(80 \text{ }^\circ\text{C}) - \nu(7.5 \text{ }^\circ\text{C})}{\nu(80 \text{ }^\circ\text{C})} \quad (4)$$

### Thermal conductivity

Results on thermal conductivity, shown in Table 3, are calculated from measured densities, heat capacities and diffusivities by applying eq. (1). It can be concluded that no significant differences in thermal conductivity of investigated paraffin wax samples had been observed. The obtained values are in reasonable agreement with the values given in Table 1, rows 2, 3, 5 and 6. Large differences of even above 100 % for thermal conductivity of C18

paraffin, shown in Table 1, row 1 are probably due to the systematic error of phase change transition interference during measurements presented in literature.<sup>11–13,23,24</sup>

The published value is obtained at 25 °C, which is very close to the melting temperature of 27.5 °C for C18 paraffin.

Generally, paraffins show poor thermal conductivities; as expected, this proved to be the greatest obstacle in employment of investigated materials as PCM. However, while in storage systems low conductivity values make low rates for heat store and release in some cases of thermal protection it is desirable to have such low values. Poor thermal conductivity of paraffin waxes could be greatly improved by preparation of composite material with a better heat-conducting material, e.g. graphite.

Considering the determined thermal properties, the following area of utilization of investigated paraffin waxes could be proposed:

- Storage of solar energy harvested by solar collector through daytime and utilization of that energy to heat water for domestic purposes during nighttime.<sup>37</sup>

- Waste heat recovery by combining air and water conditioning systems.<sup>38</sup>

- Energy storage in passive solar space and greenhouse heating systems.<sup>39,40</sup>

- Conditioning of buildings exposed to intensive solar radiation during daytime utilizing composite shutters.<sup>2</sup>

- Off peak storage of thermal energy using active floor electric heating systems. In such a manner, peak loads may be reduced and shifted to nighttime when electricity costs are lower.<sup>41,42</sup>

- Thermal protection of electronic devices from overheating, smoothing exothermic peaks in chemical reactions, heat sinks, hot pads, etc.

## Conclusion

An experimental investigation has been conducted in order to study the thermal properties of five paraffin waxes produced by INA d.d., Croatia, in order to evaluate their potential use as a phase change material. A methodology was developed and described to eliminate errors of thermophysical measurements due to phase change transitions, previously inadequately addressed in literature. The interference of the phase transition process has been indicated as a probable explanation of large differences for solid thermal conductivities and non-monotonic temperature functions reported in literature.

Thermal analysis by DSC revealed that most of the paraffin wax samples showed solid-solid transitions prior to melting. The samples melt in the temperature range between 41 to 75 °C and show total enthalpy change between  $\Delta h = 228$  and  $169 \text{ J g}^{-1}$ . Sample 46–50 absorbs and dissipates the greatest amount of energy in the investigated temperature range.

The estimation of thermal diffusivity, based on the measured temperature response and the radial heat conduction model, yielded values between  $a = 1.03$  and  $1.13 \cdot 10^{-7} \text{ m}^2 \text{ s}^{-1}$  in the temperature range of  $\vartheta = 5\text{--}10 \text{ }^\circ\text{C}$ .

Densities of solid samples, as well as the liquid density temperature dependence function, were determined. It was shown that the phase changes of paraffin waxes were associated with significant volume changes, up to 14.8 %.

The thermal conductivities were calculated from the measured heat capacities, diffusivities and densities, which gave values between  $\lambda = 0.19$  and  $0.21 \text{ W m}^{-1} \text{ K}^{-1}$ .

Despite its thermal conductivity, the investigated paraffin waxes possess satisfactory thermal characteristics for thermal energy storage applications. In order to improve their thermal conductivity and minimize volume changes, composites with a material of good thermal conductivity, e.g. graphite, should be prepared.

## ACKNOWLEDGEMENT

*The authors would like to thank Mrs. M. Jugo and Mr. Ž. Vidović from INA-Industrija nafte, d.d., Maziva, Rijeka, Croatia for providing paraffin wax samples, and Ms. Ivona Fiamengo for doing part of the DSC measurements. The financial support of the Ministry of Science, Education and Sports of Republic of Croatia within the framework of the project no. 125-1252970-2981 “Ceramic nanocomposites obtained by sol-gel process” and the project no. 125-1252970-2983 “Development of hydration process model” is greatly acknowledged.*

## Notation

### Method:

DSC – Differential scanning calorimetry

### Other used notation:

$a$  – thermal diffusivity,  $\text{m}^2 \text{ s}^{-1}$

$c_p$  – specific heat capacity,  $\text{J g}^{-1} \text{ K}^{-1}$

$h$  – specific enthalpy,  $\text{J g}^{-1}$

LHTES – latent heat thermal energy storage

- $m$  – mass of PCM used in DSC experiment, g  
 PC – personal computer  
 PCM – phase change material  
 $q$  – cumulative heats of phase transformations of paraffin waxes, J g<sup>-1</sup>  
 $Q$  – volume flow rate, mL min<sup>-1</sup>  
 $R$  – radius of specimen, mm  
 $r$  – radial dimension  
 $T$  – absolute temperature, K  
 $\dot{T}$  – heating or cooling rate of the DSC measurement, K min<sup>-1</sup>  
 $t$  – time, s  
 $v$  – specific volume, cm<sup>3</sup> g<sup>-1</sup>

#### Greeks notation:

- $\lambda$  – thermal conductivity, W m<sup>-1</sup> K<sup>-1</sup>  
 $\rho$  – density, g cm<sup>-3</sup>  
 $\sigma$  – standard deviation of temperature response fit, °C  
 $\vartheta_m$  – melting temperature (corresponding to onset of the DSC melting peak), °C  
 $\vartheta_s$  – solidification temperature (corresponding to separation of the DSC heat flow curve from the base line in the course of cooling), °C  
 $\vartheta_t$  – transition temperature corresponding to separation of the DSC heat flow curve from the base in the course of heating, °C  
 $\Phi$  – specific heat flow rate, W g<sup>-1</sup>  
 $\varphi$  – volumetric heat generation or sink, W m<sup>-3</sup>

#### References

- Farid, M. M., Khudhair, A. M., Razack, S. A. K., Al-Hallaj, S., *Energ. Convers. Manage.* **45** (2004) 1597.
- Tyagi, V. V., Buddhi, D., *Renew. Sust. Energ. Rev.* **11** (2007) 1146.
- Kurajica, S., *TehnoEko* **4** (2007) 14. (in Croatian)
- Zalba, B., Marin, J. M., Cabeza, L. F., Mehling, H., *Appl. Therm. Eng.* **23** (2003) 251.
- Himran, S., Suwono, A., Mansoori, G. A., *Energ. Source* **16** (1994) 117.
- Banu, D., Feldman, D., Hawes, D., *Thermochim. Acta* **17** (1998) 117.
- Cho, K., Choi, S. H., *Int. J. Heat Mass Tran.* **64** (2000) 37.
- Sharma, A., Sharma, S. D., Buddhi, D., *Energ. Convers. Manage.* **43** (2002) 1923.
- Akgun, M., Aydin, O., Kaygusuz, K., *Energ. Convers. Manage.* **48** (2007) 669.
- Gu, Z., Liu, H., Li, Y., *Appl. Therm. Eng.* **24** (2004) 2511.
- Abhat, A., *Sol. Energy* **30** (1983) 313.
- Sasaguchi, K., Viskanta, R., *J. Energy Resources Technol.* **111** (1989) 43.
- Dincer, I., Rosen, M. A., *Thermal energy storage, Systems and Applications*, John Wiley & Sons, Chichester England, 2002.
- Lane, G. A., *Int. J. Ambient Energy* **1** (1980) 155.
- Heckenkamp, J., Baumann, H., *Latentwärmespeicher, Sonderdruck aus Nachrichten* **11** (1997) 1075.
- Kirk-Othmer Encyclopedia of Chemical Technology, Third Edition, Vol. 24, John Wiley & Sons, New York, 1979, p. 473–476.
- Technical Bulletin – Shell Paraffin and Microcrystalline Waxes: SHELLWAX® and SHELLMAX®, Shell Lubricants, October 2000.
- North American Combustion Handbook, Second Edition, North American Mfg. Co., Cleveland, OH, 1978, p. 362.
- Properties of Non-Metallic Solids, Wattage Calculation Formulas – Paraffin Melting, Hotwatt Inc., Danvers, MA, Heaters for Every Application, www.hotwatt.com
- Chevron Refined Waxes, Chevron Lubricants, 2002.
- Buddhi, D., Sharma, A., Ramchandra, R., Balpande, A., IEA, ECESIA Annex 17, Advanced thermal energy storage through phase change materials and chemical reactions – feasibility studies and demonstration projects, 4th Workshop, 21–24 March 2003, Indore, India.
- Hamins, A., Bundy, M., Dillon, S. E., *Journal of Fire Protection Engineering* **15** (2005) 265.
- Haji-Sheikh, A., Eftekhar, J., Lou, D. Y., Vol. 82–0846, Conference: AIAA/ASME joint conference on fluids, plasma, thermophysics and heat transfer, St Louis, MO, USA, 7 Jun 1982, p. 1–7.
- Manoo, A., Hensel, E., One-dimensional two-phase moving boundary problem, HTD, Phase Change Heat Transfer, ASME **159** (1991) 97.
- Carlsaw, H. S., Jaeger, J. C., *Conduction of Heat in Solids*, 2nd Ed., Oxford University Press, London, 1959.
- Bairi, A., Laraq, N., Garcia de Maria, J. M., *J. Food Eng.* **78** (2007) 669.
- Ukrainczyk, N., *Int. J. Heat Mass Transf.* **59** (2009) 5675.
- Ukrainczyk, N., Matusinović, T., *Cem. Concr. Res.* **40** (2010) 128.
- Kakac, S., Yener, Y., *Heat Conduction*, 2nd ed., London, 1985.
- Skeel, R. D., Berzins, M., *Journal on Scientific and Statistical Computing* **11** (1990) 1.
- Shampine, L. F., Reichelt, M. W., *SIAM Journal on Scientific Computing* **18** (1997) 1.
- Craig, R. G., Powers, J. M., Peyton, F. A., *J. Dent. Res.* **46** (1967) 1090.
- Chazhengina, S. Y., Kotelnikova, E. N., Filippova, I. V., Filatov, S. K., *J. Mol. Struct.* **647** (2003) 243.
- Arkar, C., Medved, S., *Thermochim. Acta* **438** (2005) 192.
- Finke, H. L., Gross, M. E., Waddington, G., Huffman, H. M., *J. Am. Chem. Soc.* **20** (1954) 333.
- Paraffin product, Properties, Technologies, Applications, Freund, M., Csikós, R., Keszthelyi, S., Mózes, Gy., in Mózes, Gy. (Ed), *Developments in Petroleum Science 14*, Elsevier, Amsterdam, 1982.
- Vikram, D., Kaushik, S., Prashanth, V., Nallusamy, N., *Proceedings of the International Conference on Renewable Energy for Developing Countries-2006*. (<http://cere.udc.edu/An%20Improvement%20In%20The%20Solar%20Water%20Heating%20Systems%20Using%20Phas.pdf>)
- Ren-Chen, C., Sharma, A., Lan, N. V., *Phase Change Materials- a Road Map* (<http://www2.ksu.edu.tw/ksuME/ISEM/files/3eGBIC>)
- Sart, A., *Appl. Therm. Eng.* **23** (2003) 1005.
- Hadjieva, M., Stoykov, R., Filipova, T., *Renew. Energ.* **19** (2000) 111.
- Farid, M. M., Chen, X. D., *Proc. Inst. Mech. Eng.* **213** (1999) 83.
- Lin, K., Zhang, Y., Xu, X., Di, H., Yang, R., Qin, P., *Energ. Buildings* **37** (2005) 215.